Correlation Radii for Polystyrene (PS) in Poor and Θ Solvents from Dynamic Light and Small Angle Neutron Scattering. New Data for PS/Acetone. Remarks on PS/Acetone, PS/Cyclohexane, and PS/Methylcyclohexane

W. Alexander Van Hook,* Hannah Wilczura,† Attila Imre,‡ and Luis P. N. Rebelo§

Chemistry Department, University of Tennessee, Knoxville, Tennessee 37996

Yuri B. Melnichenko

Solid State Division, Oak Ridge National Laboratory, Oak Ridge, Tennessee 37831

Received February 18, 1999; Revised Manuscript Received August 7, 1999

ABSTRACT: Dynamic light scattering (DLS) and small-angle neutron scattering (SANS) correlation radii, ξ and ξ_{SANS}, are reported for polystyrene (PS)/acetone-h_6 (ACh) (DLS) and PS/ACd (DLS and SANS) solutions at near-critical concentration for ($7.5 \times 10^3 \leq M_w$/amu $\leq 25 \times 10^3$), ($0 \leq P$/MPa < 120) and ($12 \leq t$/°C ≤ 91), during pressure and temperature quenches ending at or near precipitation. The data are well described in the $(T,P)_{\psi cr}$ projection using the multidimensional reduced scaling formalism introduced previously. The analysis yields scaling exponents ($\nu \sim \nu_{SANS} = 0.65 \pm 0.06$) which are in agreement with the theoretical value, $\nu_{TH} = 0.63$, but $(\xi)^o$ and ξ_{SANS} are offset from each other, $((\xi)^o/\xi_{SANS}) \sim 3$. The superscript "o" refers to correlation radii calculated from monomodal DLS correlograms using the Stokes−Einstein relation, $(\xi)^o = k_BT/(6\pi\eta_o D)$. D is the DLS diffusion coefficient, and η_o is the pure solvent viscosity. For PS/cyclohexane (CH) and PS/methylcyclohexane (MCH) solutions, $(\xi^o/\xi_{SANS}) \sim 7$ and ~ 20, but for all three solvents, agreement improves when η_o is replaced with η, the solution viscosity. Then, $(\xi/\xi_{SANS}) \sim 0.3$, ~ 0.2, and ~ 3 for PS/AC, PS/CH, and PS/MCH, respectively. The results indicate the two probes are responding to the same or closely related clustering phenomena.

1. Introduction

We recently reported on small-angle neutron scattering (SANS) measurements of the inter- and intramolecular correlation lengths, ξ_{SANS} and $R_{g,SANS}$, of polystyrene (PS) at semidilute (near-critical) concentration in a poor solvent, acetone-d_6 (ACd), and a Θ solvent, cyclohexane-d_{12} (CHd).[1] By making use of the SANS high concentration isotope labeling method,[2−4] it is possible to determine $R_{g,SANS}$ even at entanglement concentrations and above, and at conditions close to precipitation. Conventional SANS measurements on polymer-*h* in solvent-*d* (or polymer-*d* in solvent-*h*), or dynamic light scattering (DLS) measurements on polymer-(*h* or *d*) in solvent-(*h* or *d*), yield intermolecular correlation radii, which, to preserve consistency with the earlier paper,[5] are labeled ξ_{SANS} and ξ, respectively. In an earlier report[1] we found intramolecular correlation, $R_{g,SANS}$, to be invariant during temperature or pressure quenches extending to the immediate vicinity of the (T,P) demixing locus in both ACd and Chd. That observation is indicative of the universality of the constancy of R_g, previously demonstrated[6] for Θ solvents at $T \leq \Theta$, but now extended to poor solvents. On the other hand, the intermolecular correlations diverge as critical demixing is approached during T or P quenches. Van Hook, Wilczura, and Rebelo[5] have compared ξ and ξ_{SANS} in PS/CH and PS/methylcyclohexane (MCH) solutions at near critical concentration during T and P quenches deep enough to induce LL demixing. They described the divergence of ξ and ξ_{SANS} in the $(T,P)_{\psi cr}$ plane with a multidimensional reduced scaling formalism developed for that purpose. The scaling exponents for ξ_{SANS} and ξ for PS/MCH solutions were the same within experimental error, but the DLS and SANS data were offset by more than a decade ($\xi/\xi_{SANS} \sim 20$). The present paper continues the focus on near-critical solutions, reporting ξ during T and P quenches to near precipitation in the poor solvent, acetone.

This paper is one of a series from the University of Tennessee reporting on LL demixing from weakly interacting PS solutions in small-molecule solvents over broad ranges of T and P, isotope label (H/D) on solute or solvent, concentration, molecular weight (M_w), and polydispersity.[7−11] Weakly interacting solutions are characterized by upper (UCS) and lower (LCS) two-phase consolute branches, which join at hypercritical points which may be isotope and M_w dependent. The phase diagrams have been interpreted with the aid of a continuous thermodynamic mean field algorithm[9] or (alternatively) with a scaling formalism which correlates demixing parameters with solvent quality indices.[12]

Brown and Nicolai,[13] Berry,[14] Higgins, and Benoit,[15] and des Cloizeaux and Jannink[16] have reviewed DLS and SANS techniques applied to polymer solutions. In the comparison it is important to remember that while SANS refers to a static (long time average) correlation length, DLS measurements are dynamic. They involve measurement of a relaxation time which is converted

* To whom correspondence should be addressed.

† On leave at the University of Tennessee, 1996−1998. Permanent address: Chemistry Department, University of Warsaw, Pasteura 1, 02−089 Warsaw, Poland.

‡ On leave at the University of Tennessee, 1998. Permanent address: Physical Chemistry Department, Atomic Energy Research Institute, POB 49, Budapest 1525, Hungary.

§ On leave at the University of Tennessee, 1996−1997. Permanent address: Chemistry Department, New University of Lisbon, 2825Monte da Caparica, Portugal.

10.1021/ma9902394 CCC: $18.00
Published on Web 09/30/1999

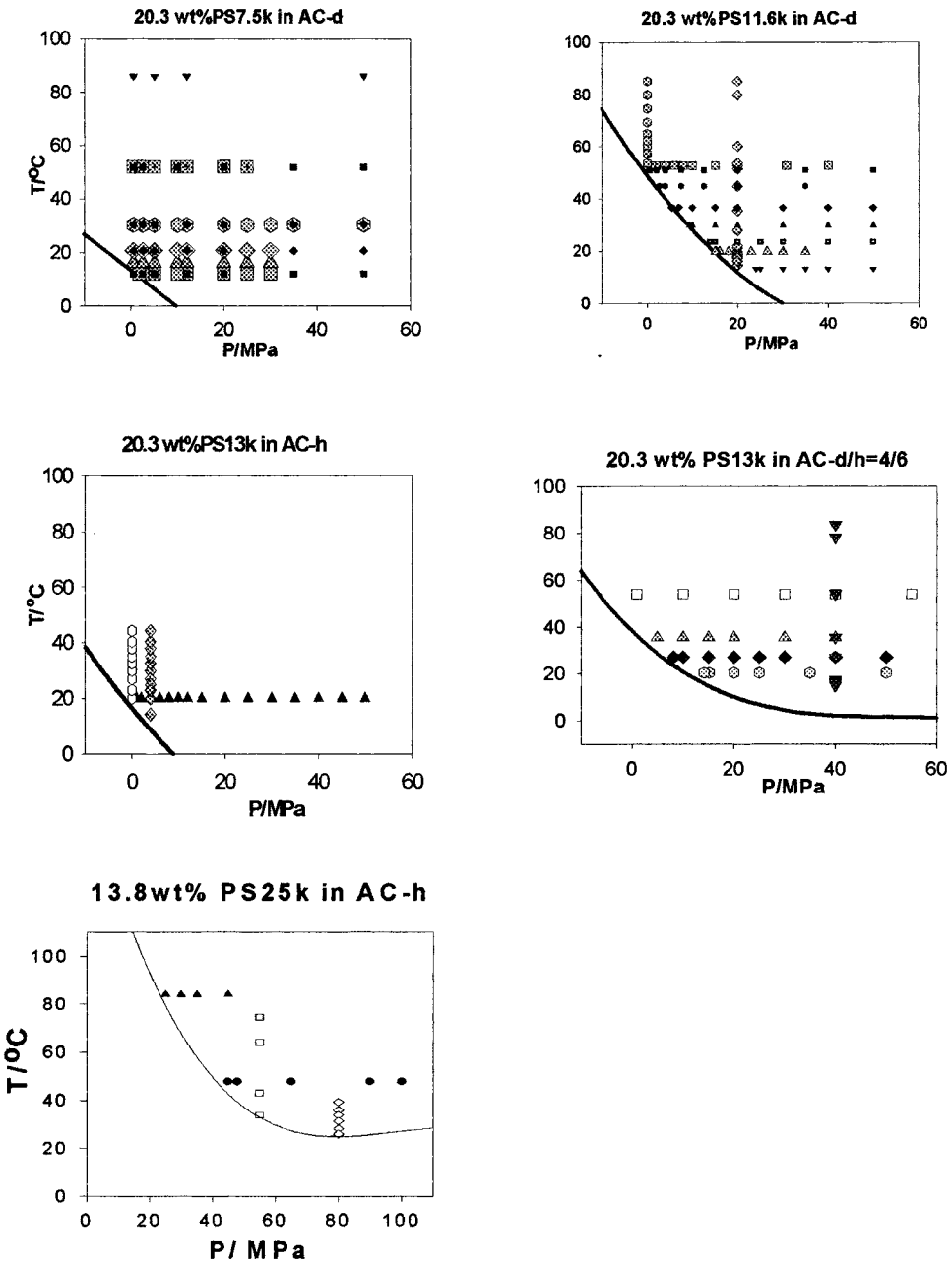

Figure 1. Location of DLS (large shaded points) and SANS (small solid points)on the LL demixing diagram (lines) of near-critical polystyrene/acetone solutions. Correlation equations are reported in Table 1. In each case the LL two phase region lies at the lower left: (a, upper left) PS7.5K/AC-*d*, 20.3 wt %; (b, upper right) PS11.6K/AC-*d*, 20.3 wt %; (c, middle left) PS13K/AC-h, 20.3 wt %; (d, middle right) PS13K/AC ($d = 40\% + h = 60\%$), 20.2 wt %; (e, lower left) PS25K/AC-*h*, 13.8 wt %. This solution was prepared under pressure.

Table 1. LL Demixing of PS/Acetone Solutions in the (*T*,*P*) Projection at Near-Critical Concentration, $T/°C = a + b(P/\text{MPa}) + c(P/\text{MPa})^2 + d(P/\text{MPa})^3$ for ($-10 \le P/\text{MPa} \le 60$)

solution	*a*	*b*	10^2c	10^4d	ref
PS13.0K/AC-*h*,20.2%	16.77	−2.166	5.70	−5.89	28
PS13.0K/AC-*h*,20.3%	16.33	−2.02	1.80		*a* (Figure 1c)
PS13.5K/AC-*h*,20.2%	24.17	−1.430	1.72	−0.81	28
PS13.0K/(AC-*h*:AC-*d*::1:1)20.2%	46.29	−2.527	5.12	−4.00	28
PS13.0K/(AC-*h*:AC-*d*::6:4)20.3%	36.30	−2.130	4.16	−2.74	*a* (Figure 1d)
PS13.0K/AC-*d*,20.2%	79.34	−3.156	4.32		28
PS11.6K/AC-*d*,20.3%	49.11	−2.314	2.27		*a* (Figure 1b)
PS7.5K/AC-*d*,20.3%	13.33	−1.362			*a* (Figure 1a)
PS25K/AC-*h*,13.8%	168.1	−4.676	4.97	−1.704	*a* (Figure 1e)

[a] This work.

to a correlation length only after the introduction of a set of assumptions relating time and distance. For solutions of low enough M_w, DLS correlograms are well described in terms of a single (monomodal) exponential decay $g_1(t)$, $g_1(t) = B \exp(-\Gamma t)$. This permits definition of $(\xi)^o$ from the cooperative diffusion coefficient of the

system, $D = \Gamma/\mathbf{q}^2$.

$$(\xi)^o = k_B T/(6\pi\eta_o D) \quad (1)$$

k_B is Boltzmann's constant and η_o the solvent viscosity. Above, B is a least-squares fitting constant, Γ is the relaxation time which describes the exponential decay, $\mathbf{q}$ the scattering vector, and t is time. Γ and thence D are obtained from the least-squares fit to the monomodal correlogram. Correlograms in Θ solvents and poor solvents are often more complex. As the concentration increases, the initially simple exponential form changes to a more complicated bimodal or polymodal pattern. The first component, a narrow peak found at a shorter time, varies linearly with $\mathbf{q}^2$ and is clearly diffusive in nature. The slow peak(s), important only at concentrations above entanglement, broaden(s) with increasing M_w and concentration as the average position shifts to longer time. The hydrodynamic correlation length, $(\xi)^o$ or ξ (vide infra), is determined from the parameters defining the short time decay.[13] The longer time relaxation process is only seen at sufficiently high viscosity.[5,13]

Equation 1, which results from application of the Stokes−Einstein relation to the DLS cooperative diffusion coefficient, $D = \Gamma/\mathbf{q}^2$, is strictly applicable only at infinite dilution because the viscosity used therein, η_o, is that for pure solvent. Nonetheless, despite cautions to the contrary,[13,17,18] eq 1 has often been applied to solutions at semidilute concentration, ordinarily using η_o (presumably because viscosity data for the solutions are unavailable), but occasionally employing solution viscosities, η. Below we compare these approaches from a strictly phenomenological point of view. Viscosities at concentrations of interest are significantly larger than pure solvent, $\eta/\eta_o \gg 1$, and we have chosen to correct $(\xi_{DLS})^o$ by writing

$$\xi = (\xi)^o(\eta_o/\eta) \quad (2)$$

The correction equation is an empirical attempt to compensate for critical slowing down[19,20] and related effects.

2. Experimental Section

High-purity polystyrene samples of low polydispersity ($M_w/M_n \leq 1.07$) were purchased from Pressure Chemical Co. and are further specified in Table 1, Supporting Information. Reagent acetone (ACh and ACd), cyclohexane (CH and Chd), and methylcyclohexane (MCHh and MCHd) were purchased from Aldrich Chemical and used as received except for drying over molecular sieve and filtration using poly(tetrafluoroethylene) 0.2 μm filters (Alltech or Whatman). DLS and SANS measurements were made using the instrument packages, pressure cells, and techniques previously described.[1,5,6] Relative viscosities, η/η_o, were determined at several temperatures and 0.1 MPa by measuring drop times for steel balls ($d \sim 0.5$ mm) in solution-filled glass capillaries ($d \sim 1$ mm). This method, which we calibrated with measurements on glycerol/water standards at 26 °C,[21] is rapid and convenient. It offers the advantage of needing only small amounts of solution (important for these expensive polymer standards and isotopically labeled solvents) but only affords a precision ~10% due to wall effects. That precision, however, is sufficient for our purpose, which is to determine whether the viscosity correction accounts for the preponderant part of observed differences between ξ_{SANS} and $(\xi_{DLS})^o$. As before we make the following strong assumption:[5,22,23] $(\eta/\eta_o)_{T,P} = (\eta/\eta_o)_{T,P=0.1}$.

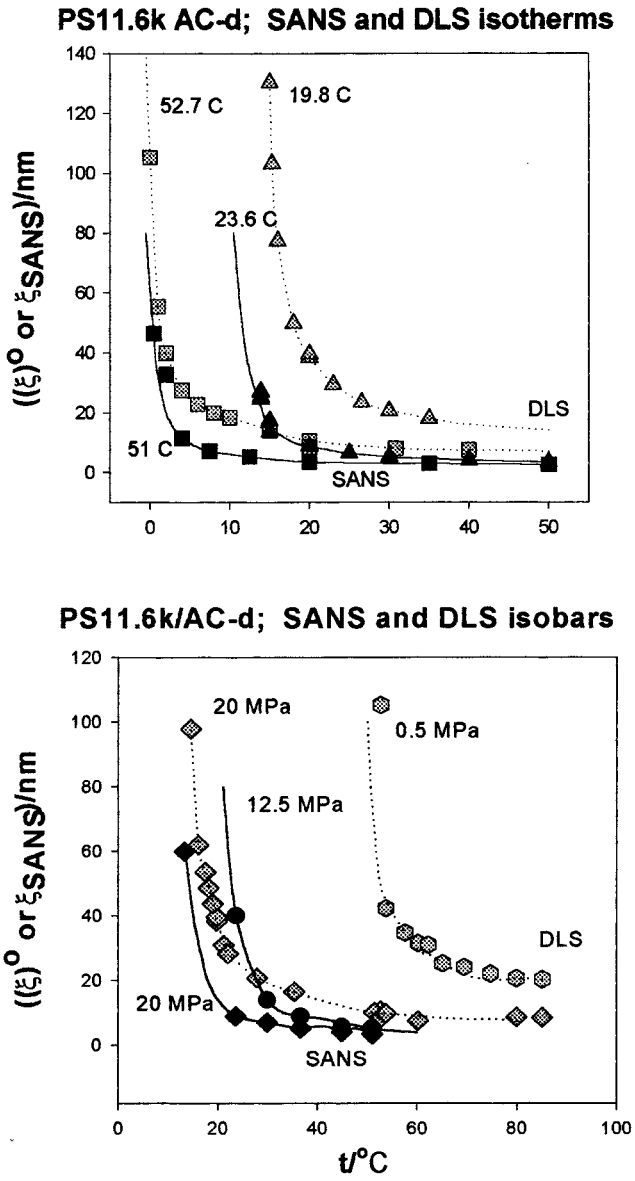

Figure 2. P and T dependences of ξ_{SANS} and $(\xi)^o$ for a near-critical PS/AC-d solution. (a, upper) Pressure dependence of ξ_{SANS} and $(\xi)^o$ in the vicinity of near-critical demixing along several isotherms. ξ_{SANS} for PS11.6K/AC-d at 51 °C (solid squares) and 23.6 °C (solid triangles);[1] $(\xi)^o$ at 52.7 (shaded squares) and 19.8 °C (shaded triangles). The data are those plotted in Figure 1b, but results at intermediate temperatures are not plotted to reduce clutter. Not shown is $R_g(P,T)$ of PS11.2K/(ACd0.79/ ACh0.21) which is equal to 2.9 nm and is T and P invariant.[1] (b, lower) Temperature dependence of ξ_{SANS} and $(\xi)^o$ in the vicinity of near-critical demixing. ξ_{SANS} for PS11.6K/AC-d at l2.5 (solid circles) and 20 MPa (solid diamonds); $(\xi)^o$ at 0.5 (shaded hexagons) and 20 MPa (shaded diamonds). The data are those plotted Figure 1b, but intermediate results are not shown here in order to reduce clutter. Not shown is $R_g(P,T)$ of PS11.2K/(ACd0.79/ACh0.21) which is equal to 2.9 nm and is T and P invariant.[1]

3. Results and Discussion

DLS and SANS for PS/AC ($0.1 \leq P/\text{MPa} \leq 120$), ($12 \leq t/\text{C} \leq 91$). Data for ξ, ξ_{SANS}, and I_{SANS}, in the (P,T) plane for PS/ACh and PS/ACd solutions at near-critical concentration (~20 wt %, $c/c^* \sim 0.2-0.4$ for ($7.5 < 10^{-3}M_w/\text{amu} < 25$), where $c^* = 3M_w/(4\pi N_{av} r_g^3)$, N_{av} is Avogadro's number, and r_g is the polymer radius of gyration) are reported in Table 1, Supporting Information. Acetone is a poor solvent, and the highest M_w in

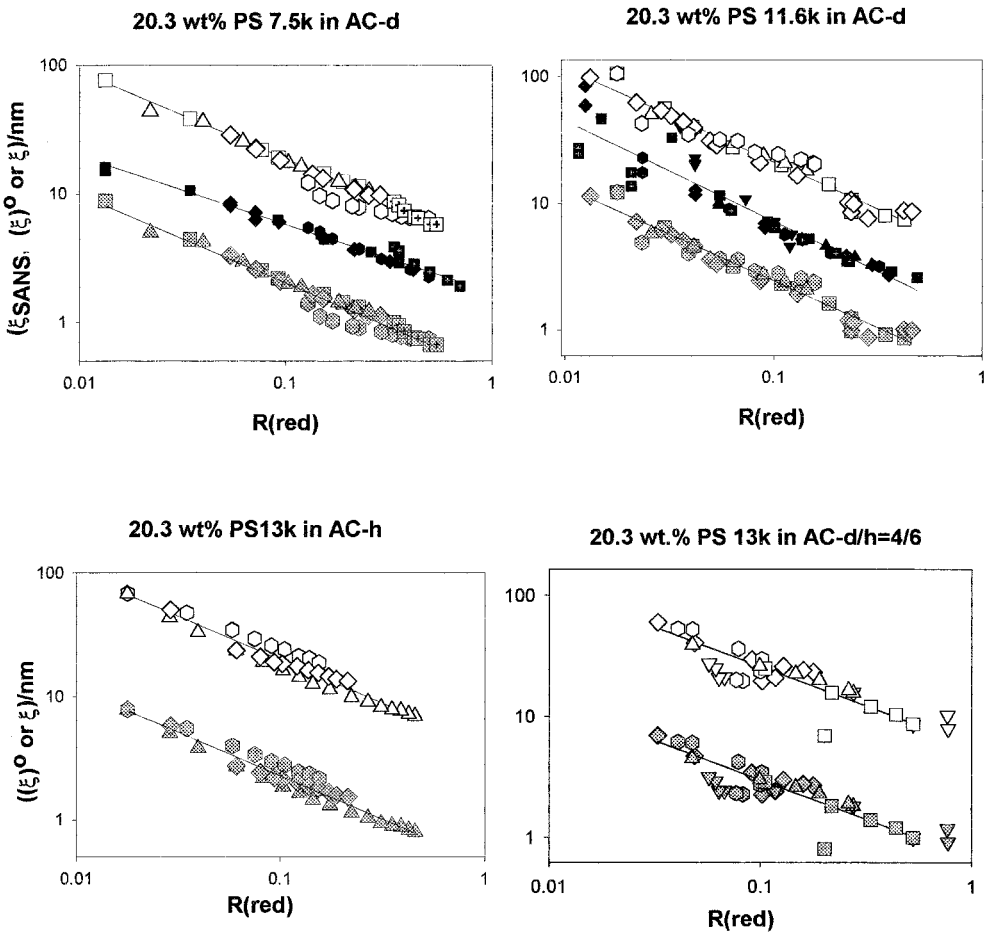

Figure 3. Scaling fits to PS/acetone data. The solutions and symbols are those of Figure 1. In each case $R_{red} = \{[(t_{exp} - t_{cr})_{min}/(t_{exp} + t^{\#})]^2 + [(p_{exp} - p_{cr})_{min}/(p_{exp} + p^{\#})]\ 2\}^{1/2}$ with $t^{\#} = 273.15$, and $p^{\#}$ (best fit) = 75 MPa. For each solution the uppermost curve (open symbols) plots $(\xi)^o$ vs R(red), the middle curve (solid symbols, if shown) plots ξ_{SANS} vs R(red), and the lowermost curve (shaded symbols) plots $\xi = (\xi)^o\ (\eta_o/\eta)$ vs R(red). Least-squares correlation lines are reported in Table 2, relative viscosities are reported in Table 3. Key: (a, upper left) PS7.5K/AC-*d*, 20.3 wt %; (b, upper right) PS11.6K/AC-*d*, 20.3 wt %; (c, lower left) PS13K/AC-*h*, 20.3 wt %; (d, lower right) PS13K/AC(d = 40% + h = 60%), 20.2 wt %.

this series is well below the value at which DLS nondiffusive slow modes develop.[5,13] Figure 1 shows the DLS and SANS data nets superposed on the LL demixing diagrams for PS/ACh and PS/ACd. Equations of the demixing correlation lines are reported in Table 1. Figure 2 illustrates the typical behavior of $(\xi)^o$ which rises toward critical divergence during pressure (Figure 2a) or temperature (Figure 2b) quenches to the immediate vicinity of the LL demixing line, comparing that behavior with ξ_{SANS} (which similarly diverges). $R_{g,SANS}$ (not shown in Figure 2) remains rock-solid invariant across the whole homogeneous portion of the (T,P) plane, even in the very near vicinity of LL demixing ($R_{g,SANS}$(PS11K/AC) = 2.7 nm).[1] The behaviors of I and I_{SANS} during T and P quenches are analogous to those for $(\xi)^o$ and ξ_{SANS}, but intensity data are neither plotted nor included in the discussion to preserve the economy of presentation. Scaling fits are discussed in a later section.

DLS and SANS for PS/CH and PS/MCH Solutions. Data nets in the (P,T) plane for $R_{g,SANS}$, ξ_{SANS}, I_{SANS}, and $(\xi)^o$ at near-critical concentration for PS/CH and PS/MCH solutions have been previously reported.[1,5,6] Table 1, Supporting Information, reports some new data for the PS/CHd system.

Both CH and MCH are Θ solvents, but CH enjoys a wider Θ gap than does MCH. In CH interpretation of scattering data in the (T,P) plane is complicated by the pressure dependent (liquid ⇒ solid) freezing curve for the pure solvent which intersects the LL demixing curve at t = 21.0 °C and P = 26.5 MPa. During P or T quenches to near demixing ξ and ξ_{SANS} for PS/CH shows near-critical divergence, but $R_{g,SANS}$ is invariant. For PS/MCH solutions ξ_{SANS} and $(\xi)^o$ diverge as demixing is approached in the (T,P) plane, and that behavior is complicated by the lower hypercritical temperature, $T_{hyp}{}^L$, found at t = 31.9 °C and P = 63.0 MPa.[5] Along isotherms close to and above $T_{hyp}{}^L$ one expects (and finds) near-critical divergence for both SANS and DLS as pressure is either lowered or raised in the approach to LL demixing. Once again, $R_{g,SANS}$ should remain invariant all the way to precipitation.[1]

Scaling Representation for DLS and SANS. Thermodynamic Equivalence of *T* and *P* Quenches to LL Demixing. Van Hook, Wilczura, and Rebelo[5] have described the development of an empirical two-dimensional scaling formalism to describe scattering data in the $(T,P)_{\psi cr}$ plane. Recognizing that at no point can the field variable describing the approach to criticality be tangent to the critical line,[24] they chose to develop scaling in terms of an empirically defined variable, R_{red}, taken as the minimum distance from the experimental point of interest to the LL critical locus in the space,

Table 2

(a) Least-Squares Fits to Eq 5, $\log(\text{correlation radius}) = \log(A) + \nu \log(R_{red})$

solution (argument)	log A	$-\nu$	r^2	$p^{\#}$	ref
PS7.5KAC-*d*,20.3%					
$(\xi)^o$	0.558	0.687	0.96	75	*a*
ξ	−0.379	0.687	0.96	75	*a*
ξ_{SANS}	0.234	0.530	0.98	75	*a*
PS11.6KAC-*d*,20.3%					
$(\xi)^o$	0.582	0.740	0.95	75	*a*
ξ	−0.355	0.740	0.95	75	*a*
ξ_{SANS}	0.063	0.793	0.89	75	*a*
PS13KAC-*h*,20.3%					
$(\xi)^o$	0.595	0.702	0.95	75	*a*
ξ	−0.341	0.702	0.95	75	*a*
PS13KAC-*d*,20.3%					
$(\xi)^o$	0.761	0.651	0.78	75	*a*
ξ	−0.176	0.651	0.78	75	*a*
all AC solutions in common					
ξ	−0.317	0.695	0.89	75	*a*
ξ_{SANS}	0.121	0.722	0.89	75	a
all MCH solutions in common					
ξ	−0.337	0.678	0.89	55	6
ξ_{SANS}	−1.019	0.750	0.84	55	6,a
all CH solutions in common					
ξ	−0.895	0.646	0.85	5500	6,b
ξ_{SANS}	−0.300	0.687	0.99	5500	1,6,b

b. Ratios of Correlation Radii.

solutions	range of R_{red}	$(\eta/\eta_o)^c$	$(\xi)^o/\xi_{SANS}$	ξ/ξ_{SANS}
AC	0.01−1	9	3	0.3
MCH	0.001−0.1	6	20	3
CH	0.005−0.1	30	7	0.2

[a] This work. [b] The large value for $p^{\#}$ for CH as compared to AC or MCH reflects the almost negligible slope of the LL demixing line,[6] $(\partial T/\partial P)_{LL} \sim 0$. [c] See Table 3d. r^2 is the statistical correlation coefficient.

$R(t,p)$

$$R_{red} = \{[(t_{exp} - t_{cr})_{min}/(t_{exp} + t^{\#})]^2 + [(p_{exp} - p_{cr})_{min}/(p_{exp} + p^{\#})]^2\}^{1/2} \quad (3)$$

The correlation radius is assumed to scale logarithmically

$$\xi = AR_{red}{}^{\nu} \quad (4)$$

In eqs 3 and 4, A is an empirical fitting parameter, ν is a scaling exponent, (t_{exp},p_{exp}) are the coordinates of an experimental point of interest, and $(t_{cr},p_{cr})_{min}$ are the coordinates of that point which lies on the critical line a minimum distance from (t_{exp},p_{exp}). The reduction parameters $t^{\#}$ and $p^{\#}$ are chosen commensurately in order to ensure that unit steps along $t_{red} = (t_{exp} - t_{cr})_{min}/(t_{exp} + t^{\#})$ and $p_{red} = (p_{exp} - p_{cr})_{min}/(p_{exp} + p^{\#})$ are thermodynamically equivalent so far as the approach to LL is concerned. This approach avoids the canonization of any point along the critical (T,P) locus as a unique scaling reference (for example a hypercritical temperature or pressure). As a consequence, in (ξ,R_{red}) space, we avoid the doubling of critical exponents implied by such selection (see refs 5 and 24 for further discussion of this important point).

Scaling fits, $\log(\xi)$ vs $\log(R_{red})$, for the acetone solutions investigated in this paper are shown in Figure 3. Least-squares regression lines for fits to eq 5 are reported in Table 2.

$$\log(\text{correlation radius}) = \log(A) + \nu \log(R_{red}) \quad (5)$$

Figure 4 collects all DLS and all SANS data for AC, CH, and MCH solutions into common representations. Least-squares regression lines are reported in Table 2.

The scaling exponents reported in Table 2 for both DLS and SANS are within experimental error (∼10%) of the theoretical value, $\nu = 0.63$,[24,25] for all three PS/solvent systems. According to Narayanan and Kumar[24] the uncertainty in ν is likely associated with the uncertainty in assignment of the critical concentrations of the solutions. The dispersions of the least-squares fits lie in the range 0.1−0.2 $\log(R_{red})$ units. For each solvent system, the DLS and SANS plots, while parallel, are offset from each other by factors which vary from 3 (in AC) to 20 (MCH). It was this observation which led us to apply viscosity corrections to the $(\xi_{DLS})^o$ data. The viscosity results, all of which refer to solutions of near-critical concentration, are reported in Table 3. The

Table 3. Viscosity Corrections

(a) Smoothing Relations for Solvent Viscosities, $\log(\eta_o/\text{CP})_{0.1MPa} = A + B/(T/\text{K}) + C(T/\text{K}) + D(T/\text{K})^2$

material	A	B	10^2C	10^5D	ref
AC-*h*	−7.2126	903.05	1.8385	−2.0353	29
MCH-*h*	−1.9879	508.06	0.12152	−0.27318	29
CH-*h*	4.7423	−253.22	−1.6927	1.2472	29

(b) Pressure Dependence, $\log(\eta_p/\eta_{0.1MPa}) = (E + F\Theta)(P/\text{MPa}) + (G + H\Theta)(P/\text{MPa})^2$

material	Θ	E	F	G	H	ref
AC-*h*	30	1.668×10^{-3}	0	-5.788×10^{-7}	0	30
MCH, CH	$(t/°C - 30)$	3.6367×10^{-3}	-1.12×10^{-5}	-8.7347×10^{-7}	5.3910×10^{-9}	5, 30

(c) Isotope Effects on Viscosity

material	η_o(perdeutero)/η_o(perprotio)	ref
AC	not available (∼1.00?)	
CH (and MCH)	1.06	31

(d) Falling Ball Viscosity Ratios $(\eta/\eta_o)_{0.1MPa}$ Determined in This Work: η_o = Solvent Viscosity

solution	t/°C	η/cP	η/η_o	solution	t/°C	η/cP	η/η_o
PS30K/MCH-*h*11.5 wt %	57	2.3	4.9	PS90K/CH13.1 wt %	36	23	37
	38	3.3	5.7		31	26	31
	35	3.6	5.9	PS13K/AC-*h*20 wt %	41	2.3	8.6
PS90K/CH13.1 wt %	61	13	24		36	2.4	8.6
	51	16	26		32	2.5	8.7
	41	20	28		26	2.6	8.7

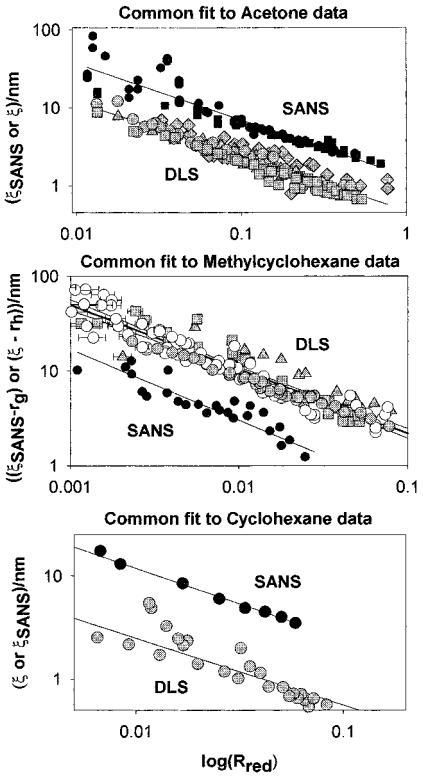

Figure 4. Scaling fits to DLS (viscosity corrected) and SANS data in PS/AC, PS/MCH and PS/CH solutions, all MW's. (a, top). PS/AC SANS (solid symbols) and PS/AC DLS (shaded symbols), $p^{\#}$= 75 MPa. SANS: Solid circles = PS11.6K in AC-*d*; solid squares = PS7.5K in AC-*d*. DLS: Shaded circles = PS11.6K in AC-*d*; shaded squares = PS7.5K in AC-*d*; shaded diamonds = PS13K in AC-*d*; shaded triangles = PS13K in AC-*h*. Correlation lines are reported in Table 2. The ratio of correlation lengths is $x_{DLS}/x_{SANS} \sim 0.3$. (b, middle). PS/MCH SANS (solid symbols) and PS/MCH DLS (shaded symbols) correlation radii, $p^{\#}$= 55 MPa. SANS: Solid circles = PS30K in MCH-*d*. DLS: Open circles = PS30K in MCH-*d*; shaded circles = PS30K in MCH-*h*; shaded squares = PS90K in MCH-*h*; shaded triangles = PS400K in MCH-*h*. The DLS data are from ref 6. Correlation lines are reported in Table 2. The ratio of correlation lengths is $\xi/\xi_{SANS} \sim 3$. (c, bottom). PS/CH SANS (solid symbols) and PS/CH DLS (shaded symbols) correlation radii, $p^{\#}$= 5500 MPa.[23] SANS: solid circles = PS115K in CH-*d*.[24] DLS: shaded circles = PS90K in MCH-*h*. The DLS data are from ref 6. Equations of the correlation lines are reported in Table 2. The ratio of correlation lengths is $\xi/\xi_{SANS} \sim 0.2$

resulting corrections to $(\xi)^o$ are approximate as they assume eq 2 and the additional strong approximation $(\eta/\eta_o)_{T,P,\psi cr} = (\eta/\eta_o)_{T,P=0.1,\psi cr}$. Nonetheless, as shown in Figure 4, the corrected DLS data in each of the three solvents now fall into approximate agreement with the SANS results (i.e., within a factor of ~3), and in each case, this holds over nearly 100-fold changes in R_{red}. We find it interesting that the ratio ξ/ξ_{SANS} is nearly the same for CH, MCH, and AC ($\sim 0.3 \leq \xi/\xi_{SANS} \leq \sim 3$), in each case over a wide change in R_{red}, even though the ratio of wavelengths of the probe radiations is more than 10^3 ($\lambda/\lambda_{SANS} = 1332$).[26] We conclude the two techniques are measuring identical or at least closely related structural correlations.

Acknowledgment. The work at the University of Tennessee was supported by the U.S. Department of Energy, Division of Materials Sciences (DE88ER45374), and at Oak Ridge National Laboratory by the U.S. Department of Energy, Division of Materials Sciences under Contract No. DE-AC05-96OR-22464 (with Lockheed Martin Energy Research Corp.).

Supporting Information Available: Table of DLS and SANS data. This material is available free of charge via the Internet at http://pubs.acs.org.

References and Notes

(1) Melnichenko, Y. B.; Wignall, G. D.; Van Hook, W. A.; Szydlowski, J.; Wilczura, H.; Rebelo, L. P. N. *Macromolecules* **1998**, *31*, 8436.
(2) Williams, C. E.; Nierlich, M.; Cotton, J. P.; Jannink, G.; Boue, F.; Daoud, M.; Farnoux, B.; Picot, C.; de Gennes, P.-G.; Rinaudo, M.; Moan, M.; Wolf, C. *J. Polym. Sci., Polym. Lett. Ed.* **1979**, *17*, 379.
(3) Akasu, A. Z.; Summerfield, G. C.; Jahansan, S. N.; Han C. C.; Kim, C. Y.; Yu, H. J. *Polym. Sci., Polym. Phys. Ed.* **1980**, *18*, 863.
(4) King, J. S.; Boyer, W.; Wignall, G. D.; Ullman, R. *Macromolecules* **1985**, *18*, 709.
(5) Van Hook, W. A.; Wilczura, H.; Rebelo, L. P. N. *Macromolecules* **1999**, *32*, 7299.
(6) Melnichenko, Y. B.; Wignall, G. D. *Phys. Rev. Lett.* **1997**, *78*, 686.
(7) Szydlowski, J.; Van Hook, W. A. *Macromolecules* **1991**, *24*, 4883.
(8) Luszczyk, M.; Rebelo, L. P. N.; Van Hook, W. A. *Macromolecules* **1995**, *28*, 745.
(9) Luszczyk, M.; Van Hook, W. A. *Macromolecules* **1996**, *29*, 6612.
(10) Imre, A.; Van Hook, W. A. *J. Polym. Sci., Polym. Phys.* **1996**, *34B*, 751.
(11) Imre, A.; Van Hook, W. A. *J. Polym. Sci., Polym. Phys.* **1994**, *32B*, 2283.
(12) Imre, A.; Van Hook, W. A.: *J. Phys. Chem. Ref. Data.* **1996**, *25*, 637.
(13) Brown, W.; Nicolai, T. In *Dynamic Light Scattering. The method and some applications*; Brown, W., Ed.; Clarendon Press: Oxford, England, 1993; Chapter 6 pp 272−318.
(14) Berry, G. C. *Adv. Polym. Sci.* **1994**, *114*, 233.
(15) Higgins, J. S.; Benoit, H. C. *Polymers and Neutron Scattering*; Clarendon Press: Oxford, England, 1994.
(16) Des Cloizeaux, J.; Jannink, G. *Polymers in Solution. Their Modeling and Structure*; Claredon Press: Oxford, England, 1990.
(17) Gold, D.; Onyenemezu, C.; Miller, W. G. *Macromolecules* **1996**, *29*, 5700.
(18) Sun, S. F. *Physical Chemistry of Macromolecules*; John Wiley and Sons: New York, 1994, Chapter 10.
(19) Jian, T.; Vlassopoulos, D.; Fytas, G.; Pakula, T.; Brown, W. *Colloid Polym. Sci.* **1996**, *274*, 1033.
(20) Ikier, C.; Klein, H.; Woermann, D. *Macromolecules* **1995**, *28*, 1003.
(21) Hogeman, C. D., Ed. *Handbook of Chemistry and Physics*, 35th ed.: CRC Press: Cleveland, OH, 1953.
(22) Beiner, M.; Fytas, G.; Meier, G.; Kumar, S. K. *Phys. Rev. Lett.* **1998**, *81*, 594.
(23) Cook, R. L.; King, H. E., Jr.; Peiffer, D. G. *Phys. Rev. Lett.* **1992**, *69*, 3072.
(24) Narayanan, T.; Kumar, A. *Phys. Rep.* **1994**, *249*, 135.
(25) LeGuillou, J. C.; Zinn-Justin, J. *J. Phys. (Paris)* **1989**, *50*, 1365.
(26) Other estimates of this ratio can be obtained. From the review of Fetters, Hadjichristidis, Lindner, and Mays (*J. Phys. Chem. Ref. Data* **1994**, *23*, 619) $R_g/R_h = 1.36 \pm 0.15$ for PS dissolved in a series of solvents (nominally at room temperature), which, using ($R_g \sim \xi_{static}\, 3^{1/2}$),[1, 16] gives ($R_h/\xi_{static} \sim \xi/\xi_{static} \sim 1.3 \pm 0.2$). This estimate is low because $\xi_{DLS} \sim R_h$ only in the limit of low concentration, and ξ increases with concentration. Brown and Nicolai in their 1990 paper (*Colloid Polym. Sci.* **1990**, *268*, 977) present correlating fits of light scattering data which yield $\xi_{static}/\xi_{DLS} = 0.5 \pm 0.3$ ($1.2 < \xi_{DLS}/\xi_{static} < 4$). One of us (YM) advocates $(\xi_{DYNAMIC}/\xi_{STATIC})_\Theta \sim 3-3.5$ under Θ conditions. The above estimates are for solutions under Θ or better than Θ conditions, but the present experiments lie well to the poor solvent side of Θ and this may affect the ratio. Viscosity corrected ratios, ξ_{DLS}/ξ_{SANS}, in Table 2b are below the lower limit of the range calculated from the light-scattering data for AC and CH, but near midrange for MCH solutions. A helpful comment from one

reviewer points out the ratio should be close to 1, if the mesh size (which depends on c/c^*) can be neglected.
(27) See footnote b, Table 2.
(28) Imre, A.; Melnichenko, G.; Van Hook, W. A. *Phys. Chem.-Chem. Phys.* **1999**, *1*, 4287.
(29) Yaws, C. L. *Handbook of Viscosity*; Gulf Publishing Co.: Houston, TX, 1995.
(30) Bridgeman, P. W. *The Physics of High Pressure*; G. Bell and Sons: London, 1958.
(31) Rabinovitch, I. B. *Influence of Isotopy on the Physicochemical Properties of Liquids*; Consultants Bureau: New York 1970.

MA9902394